

High-gain ultra-wideband bismuth-doped fiber amplifier operating in the O + E + S band

ZIWEI ZHAI*  AND JAYANTA K. SAHU 

Optoelectronics Research Centre, University of Southampton, Highfield, Southampton SO17 1BJ, UK

*z.zhai@soton.ac.uk

Received 3 April 2024; revised 21 May 2024; accepted 22 May 2024; posted 23 May 2024; published 3 June 2024

We present a double-pass bismuth (Bi)-doped fiber amplifier (BDFA) providing high-gain wideband amplification from 1330 to 1480 nm. A peak gain of 38 dB with 4.7 dB noise figure (NF) was obtained at 1420 nm for a -23 dBm input signal, with >20 dB gain from 1335 to 1475 nm. We achieved 30 and 21.5 dB peak gains with 122 nm (1341–1463 nm) and 140 nm (1333–1473 nm) 6 dB-gain bandwidth for -10 and 0 dBm input signal, respectively. For a 0 dBm signal, the power conversion efficiency (PCE) reached 23.7%, and the in-band optical-signal-to-noise ratio (OSNR) across the wideband BDFA was >44 dB. Also, the absorption and luminescence characteristics have been studied for different Bi-doped phosphosilicate fibers (BPSFs) fabricated in-house.

Published by Optica Publishing Group under the terms of the [Creative Commons Attribution 4.0 License](https://creativecommons.org/licenses/by/4.0/). Further distribution of this work must maintain attribution to the author(s) and the published article's title, journal citation, and DOI.

<https://doi.org/10.1364/OL.525583>

Introduction. Bismuth (Bi)-doped fiber (BDF) has emerged as an active area of research focus owing to its remarkable ultra-wide near-infrared (NIR) luminescence from various Bi active centers (BACs), covering from 1150 to 1500 nm and 1600 to 1700 nm [1]. The formation of NIR-emitting BACs strongly depends on the glass compositions, where effective Bi-doped fiber amplifiers (BDFAs) have been reported using Bi-doped phosphosilicate fibers (BPSFs) in the O and E bands [2,3], Bi-doped germanosilicate fibers (BGSFs) in the E and S bands [4–6], and Bi-doped high-Ge (≥ 50 mol%) germanosilicate fibers in the U band [7]. The highest gain of BDFAs reported to date is ~ 40 dB for a small input signal when using BPSF in the O-band BDFA [2] and using BGSF in the E-band BDFA [4–6]. Recently, there have been successful demonstrations of the wideband BDFA covering the O + E band. In 2020, we demonstrated an ultra-broadband BDFA, exhibiting a ~ 30 dB peak gain and >20 dB gain in a 115 nm bandwidth for a -23 dBm input signal using 220 m of BPSF [8]. For a -10 dBm input signal, the peak gain was ~ 26 dB with a pump-to-signal power conversion efficiency (PCE) of $<5\%$. In 2021, a 116 nm bandwidth BDFA was reported, providing >23 dB gain with ~ 26 dB peak gain for a -25 dBm input signal using 150 m of BPSF, where the PCE is $\sim 5\%$ and $\sim 11\%$ for an input signal of -10 and 0 dBm,

respectively [9]. In 2022, by combining BPSF with BGSF and utilizing gain clamping at 1280 nm, a 150 nm 6 dB-gain bandwidth BDFA was demonstrated with a peak gain of ~ 24 dB for a -25 dBm input signal, at the expense of a significantly higher pump power of 2.75 W [10]. However, the wideband gain achieved to date is still ~ 10 dB lower than that of the individual O-band and E-band BDFAs [2,4,5,6].

In this paper, we present a high-gain ultra-wideband BDFA operating from 1330 to 1480 nm covering from O- across E- up to the S band. By tailoring the glass host to balance the BACs associated with P (BACs-P) and BACs associated with Si (BACs-Si), a BPSF with ~ 4 mol% of P_2O_5 was demonstrated as a suitable candidate offering a wideband amplification. Using a double-pass and dual-pump amplifier configuration, we achieved a peak gain of 38 dB with a NF of 4.7 dB at 1420 nm for an input signal of -23 dBm. For input signals of -10 and 0 dBm, we obtained peak gains of 30 dB and 21.5 dB, with corresponding NFs of 5.8 and 7.5 dB, along with 6 dB-gain bandwidths of 122 nm (1341–1463 nm) and 140 nm (1333–1473 nm). The in-band optical-signal-to-noise ratio (OSNR) was measured to be greater than 22, 34, and 44 dB across the entire operating bandwidth of the amplifier when subjected to an input signal of -23 , -10 , and 0 dBm, respectively. Furthermore, a power conversion efficiency (PCE) of 23.7% has been reached for an input signal of 0 dBm. To the best of our knowledge, we present a wideband BDFA with the highest gain and PCE for input signals considered within the scope of this work.

Fiber characteristics. The Bi-doped phosphosilicate preform was fabricated in-house using the modified chemical vapor deposition (MCVD) and solution doping technique, then drawn into a fiber (BPSF-1) with a core/cladding diameter of $\sim 10/150$ μm , a refractive index difference (dn) of ~ 0.0038 , and an LP_{11} cut-off of ~ 1100 nm. The P_2O_5 concentration was measured to be ~ 4 mol% by the electron probe micro analyzer (EPMA). The small-signal absorption measured by the cutback method was 0.91 and 0.88 dB/m at the pump wavelength of 1270 and 1310 nm, respectively. The unsaturable loss (UL) was measured to be $\sim 15\%$ at 1270 nm and $\sim 11\%$ at 1310 nm. The background loss was found to be ~ 0.01 dB/m at 1550 nm, with an estimated OH concentration of 0.6 ppm. For a comparative study, another in-house fabricated BPSF-2 was selected. BPSF-2 has a dn of ~ 0.0055 , a background loss of ~ 0.04 dB/m, an absorption of 0.55 dB/m (0.46 dB/m) at 1270 nm (1310 nm), a UL of 13.5% (11.6%) at 1270 nm (1310 nm), and an estimated OH content of 0.8 ppm. The P_2O_5 concentration was

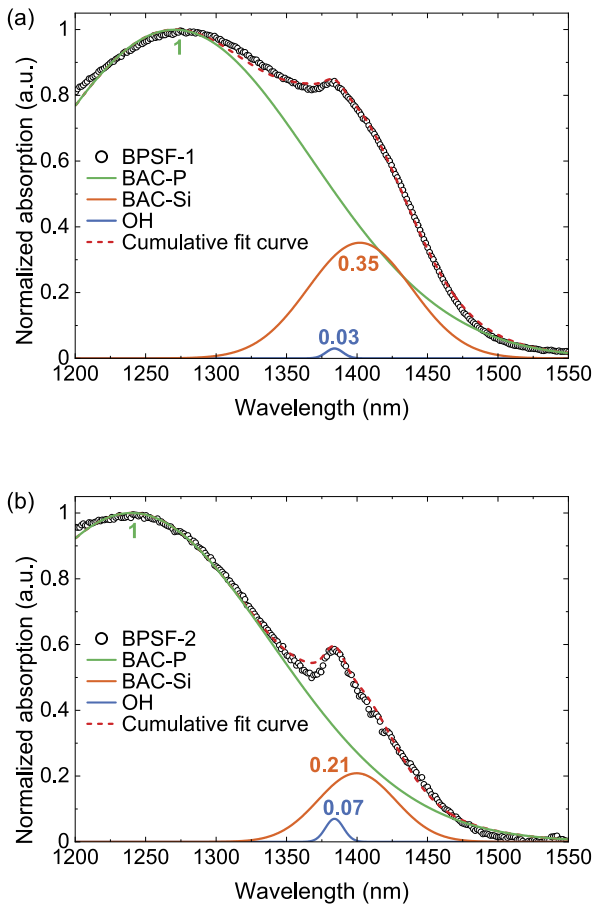


Fig. 1. Gaussian peak fittings to the normalized absorption curve of (a) BPSF-1 and (b) BPSF-2. The peak amplitude of each band is presented.

estimated to be 5.8 mol% in BPSF-2. Figures 1(a) and 1(b) show the normalized absorption spectra of BPSF-1 and BPSF-2 after subtracting the background loss. The normalized absorption was decomposed into multiple overlapping Gaussian peaks related to BACs-P (~1250 nm), BACs-Si (~1400 nm), and OH (~1385 nm), respectively [11]. With the same peak amplitude of the 1250 nm-BAC-P band, the peak amplitude of the 1400 nm-BAC-Si band is higher in BPSF-1 compared to BPSF-2, with values of 0.35 and 0.21, respectively. Accordingly, a larger fraction of effective BACs-Si sites is expected in BPSF-1. Figures 2(a) and 2(b) show the normalized luminescence spectra excited at 1310 nm of BPSF-1 and BPSF-2, decomposed into two Gaussian peaks related to BACs-P (~1300 nm) and BACs-Si (~1420 nm), respectively [12]. In the phosphosilicate host glass, BACs-P mainly contribute to the O-band gain, while BACs-Si primarily enhance the E-band gain. Compared to BPSF-2, BPSF-1 exhibits a larger fraction of BACs-Si and more balanced peak amplitudes of the two overlapping bands. This characteristic makes BPSF-1 well-suited for combining the operating wavelengths associated with BACs-P and BACs-Si, i.e., developing a wideband amplifier [11].

O + E + S band amplifier. Figure 3 illustrates the experimental setup of the double-pass BDFA by applying two circulators (CIRs, Lightel Technologies-polarization insensitive optical circulator). The loss of the circulator was measured to be 0.80 ± 0.55 dB from 1330 to 1480 nm. The fiber length

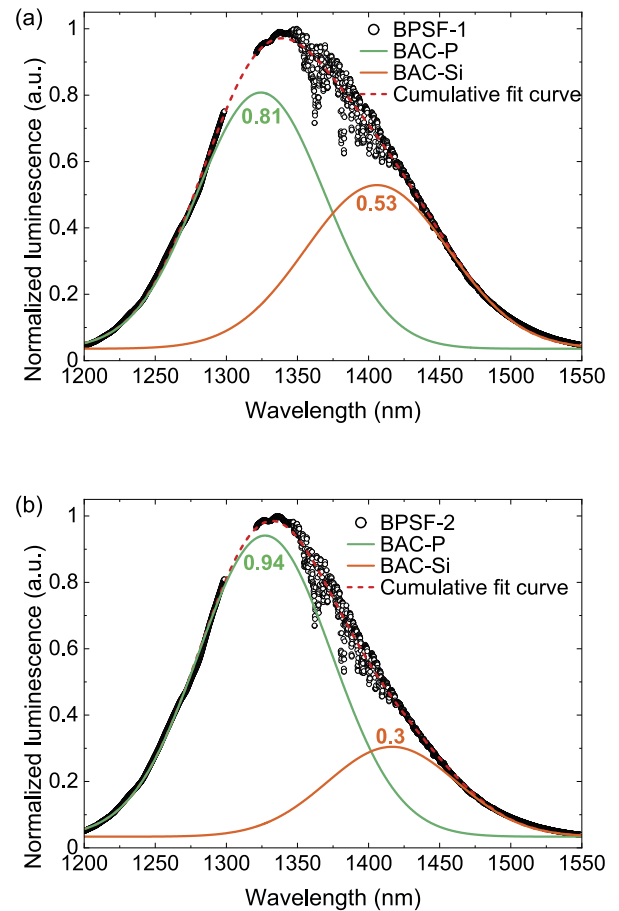


Fig. 2. Gaussian peak fittings to the normalized luminescence curve measured under the 1310 nm excitation of (a) BPSF-1 and (b) BPSF-2. The peak amplitude of each band is presented.

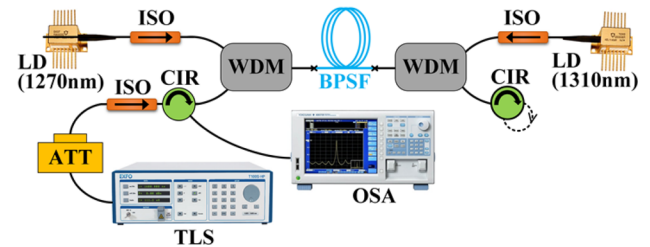


Fig. 3. Schematic of the experimental setup of the double-pass O + E + S-band BDFA.

was optimized with respect to the highest peak gain and low NF, which was 117 m for BPSF-1 and 195 m for BPSF-2. A dual-pump of 1270 + 1310 nm was utilized to optimize the gain flatness for wideband amplification. For BPSF-1, the optimal pump configuration was 400 mW from the 1270 nm laser diode (LD) and 200 mW from the 1310 nm LD. For BPSF-2, 380 mW pump power from the 1270 nm LD and 624 mW pump power from the 1310 nm LD were utilized. The pump power was optimized with respect to a more balanced gain peak at ~1370 and ~1420 nm, thus achieving an improved gain flatness. A tunable laser source (TLS) was used to provide the signals from 1330 to 1480 nm with an attenuator (ATT) to help adjust the signal power. Three isolators (ISOs) were used to prevent

back reflections. Two wavelength division multiplexers (WDMs, Lightel Technologies-filter WDM) were used to couple and separate the signal and pumps. The loss of the WDM was measured to be 0.70 ± 0.04 dB from 1330 to 1480 nm. An optical spectrum analyzer (OSA, Yokogawa-AQ6370) was used to capture the input and output signal spectra with a resolution bandwidth

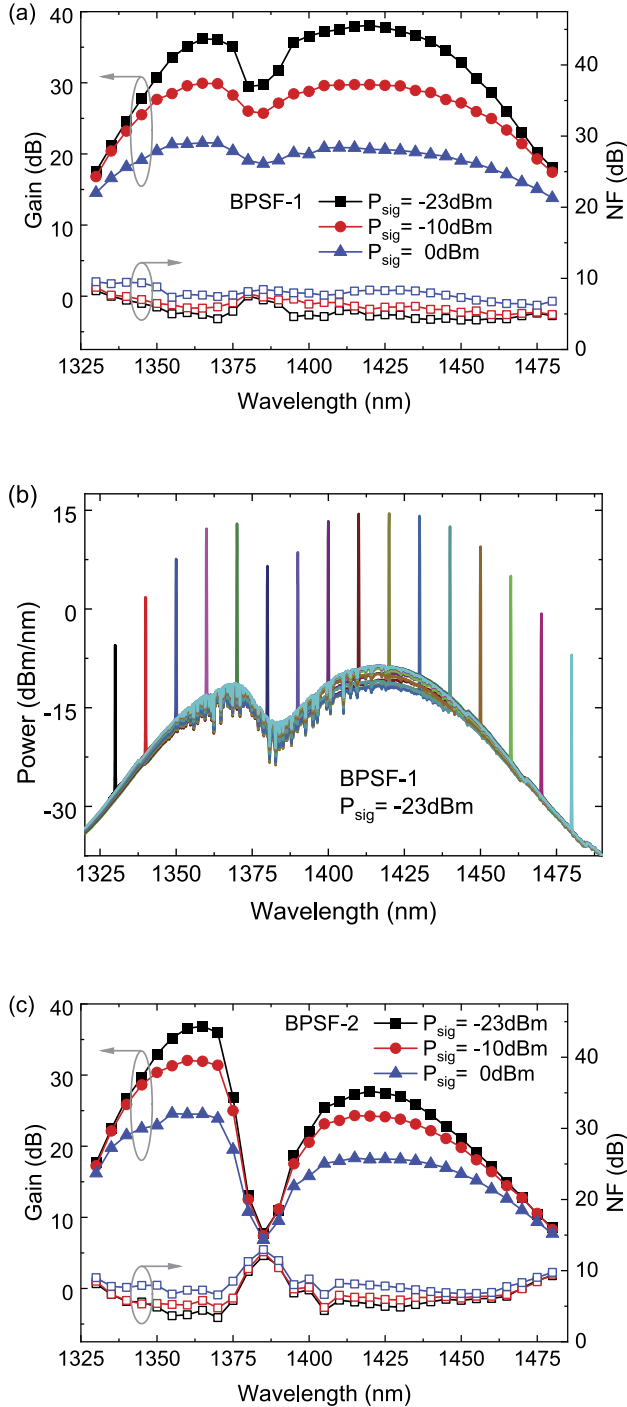


Fig. 4. (a) Gain and NF spectra from 1330 to 1480 nm for different input signal powers of 117 m of BPSF-1 with a total pump power of 600 mW. (b) Signal and noise spectra measured from 117 m of BPSF-1 for a -23 dBm input signal, from which the in-band OSNR was derived. (c) Gain and NF spectra from 1330 to 1480 nm for different input signal powers of 195 m of BPSF-2 with a total pump power of 1004 mW.

of 0.2 nm. The component loss was considered in the gain and noise figure (NF) calculations.

Figure 4(a) presents the gain and NF spectra of BPSF-1 from 1330 to 1480 nm for an input signal power of -23 , -10 , and 0 dBm, respectively. For a -10 dBm signal, the BDFAs provided a wideband amplification with >20 dB gain over 138 nm bandwidth from 1335 to 1473 nm and the average NF was ~ 6.3 dB. A 6 dB-gain bandwidth of 122 nm from 1341 to 1463 nm was demonstrated with a peak gain of 30 dB, which was comparable to the highest gain reported in individual O-band and E-band BDFAs [2,4,5,6]. For a 0 dBm signal, a 6 dB-gain bandwidth of 140 nm from 1333 to 1473 nm was achieved with a peak gain of 21.5 dB. For a -23 dBm signal, a 38 dB peak gain was obtained with a 4.7 dB NF at 1420 nm. We achieved a >20 dB gain from 1335 to 1475 nm and ~ 5.3 dB average NF. The wideband gain level has been improved for ~ 10 dB with the NF left at a similar level as the reported wideband O + E-band BDFAs [8–10]. The highest PCE was found to be 5.7%, 16%, and 23.7% for an input signal of -23 , -10 , and 0 dBm, respectively. Figure 4(b) illustrates the signal and noise spectra for a -23 dBm input signal, from which the in-band OSNR was derived. The in-band OSNR was found to be >22 dB, >34 , and >44 dB across the entire operating band for an input signal of -23 , -10 , and 0 dBm, respectively. The key parameters of the peak gain, corresponding NF and PCE, and the 6 dB-gain bandwidth are presented in Table 1 for different input signal powers.

It is worth mentioning that by increasing the total pump power to ~ 1 W (400 mW pump power from the 1270 nm LD and 624 mW pump power from the 1310 nm LD), we can achieve a maximum gain of >43 dB with a 5.4 dB NF, appearing at 1420 nm for a -23 dBm input signal power. This enhancement in gain is particularly pronounced in the E band, with minimal compromise to the O-band gain.

Table 1. Main Amplifier Parameters of BPSF-1 for Different Input Signal Powers

P_{sig} (dBm)	Gain (dB)	NF (dB)	PCE	6 dB-Gain Bandwidth (nm)
-23	38	4.7	5.7%	60
-10	30	5.8	16%	122
0	21.5	7.5	23.7%	140

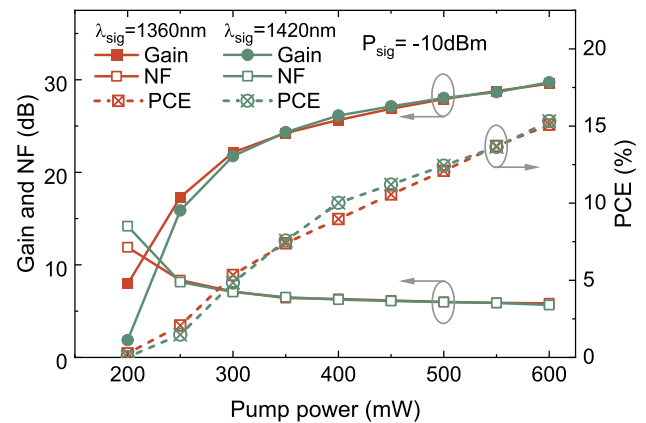


Fig. 5. Gain, NF, and PCE variations with the total pump power for a -10 dBm input signal at 1360 and 1420 nm.

For BPSF-2, the gain and NF spectra were presented in Fig. 4(c) for an input signal power of -23 , -10 , and 0 dBm, respectively. A comparable O-band gain was obtained as in BPSF-1. However, there was a noticeable gain drop in the E + S band, with a 9 dB drop from the peak gain in the O band to the peak gain in the E + S band for a -23 dBm input signal. The peak gain difference was ~ 8 dB for a -10 dBm input signal and ~ 6 dB for a 0 dBm input signal. It is mainly due to the significant excess of BACs-P over BACs-Si in BPSF-2 (as illustrated in Figs. 1 and 2), limiting its E + S-band amplification.

In addition, the gain, NF, and PCE variations with the total pump power were measured at 1360 and 1420 nm for BPSF-1. Figure 5 presents the results for a -10 dBm input signal, where the gain and NF increased, and the NF decreased with the pump power. The gain coefficient (the highest ratio of the gain to the pump power) was ~ 0.074 dB/mW at 1360 and 1420 nm for a -10 dBm signal and ~ 0.086 and ~ 0.05 dB/mW for -23 and 0 dBm signal, respectively.

Conclusions. We experimentally proved the suitability for wideband amplification from a BPSF fabricated in-house in the tailored glass host with balanced BACs-P and BACs-Si. We successfully demonstrated a high-gain wideband BDFA operating from 1330 to 1480 nm in the double-pass and dual-pump configuration utilizing the pump wavelengths of $1270 + 1310$ nm with an optimized pump power of $400 + 200$ mW for 117 m of BPSF-1. A 30 dB peak gain with a 122 nm 6 dB-gain bandwidth from 1341 to 1463 nm was achieved for a -10 dBm input signal. A peak gain of 38 and 21.5 dB was achieved for the -23 and 0 dBm input signal, respectively. It is, to the best of our knowledge, the highest reported gain from wideband BDFAs. A 140 nm 6 dB-gain bandwidth from 1333 to 1473 nm with the highest PCE of 23.7% was achieved for a 0 dBm input signal. Moreover, the absorption and luminescence characteristics of two BPSFs were investigated, revealing more balanced BACs-P and BACs-Si effectively improved the wideband amplification capacities in BPSF-1. It is worth mentioning that the dip at ~ 1385 nm between the two gain humps was compromised by the OH absorption band, which was estimated to be 3.5 dB over the 117 m long fiber. No specific measures have been undertaken to reduce the OH content in the current generation of BDFs, which will be addressed effectively by improving the drying process

during the preform fabrication. The reported BDFA holds significant promise for applications in WDM data transmission covering the O + E + S band in existing SMF infrastructure or over hollow-core NANFs (nested anti-resonant nodeless fibers) supporting ultra-wide bandwidth.

Funding. Engineering and Physical Sciences Research Council (EP/P030181/1).

Disclosures. The authors declare no conflicts of interest.

Data availability. The data for this work are accessible through the University of Southampton Institutional Research Repository [13].

REFERENCES

1. Y. Wang, S. Wang, A. Halder, *et al.*, *Opt. Mater. Express* **17**, 100219 (2023).
2. N. K. Thipparapu, Y. Wang, A. A. Umnikov, *et al.*, *Opt. Lett.* **44**, 2248 (2019).
3. Y. Wang, N. K. Thipparapu, D. J. Richardson, *et al.*, in *Optical Fiber Communication Conference (OFC) 2021*, OSA Technical Digest (Optical Society of America, 2021), paper Tu1E.1.
4. Z. Zhai, A. Halder, and J. K. Sahu, in *European Conference on Optical Communication (ECOC) (2023)*, paper Th.C.1.1.
5. S. Liu, X. Yin, Z. Gu, *et al.*, *Opt. Lett.* **49**, 314 (2024).
6. A. Donodin, E. Manuylovich, V. Dvoyrin, *et al.*, *APL Photonics* **9**, 046102 (2024).
7. S. V. Firstov, S. V. Alyshev, K. E. Riumkin, *et al.*, *J. Sel. Top. Quantum Electron.* **24**, 1 (2018).
8. Y. Wang, N. K. Thipparapu, D. J. Richardson, *et al.*, *J. Lightwave Technol.* **39**, 795 (2021).
9. Y. Ososkov, A. Khagai, S. Firstov, *et al.*, *Opt. Express* **29**, 44138 (2021).
10. A. Khagai, Y. Ososkov, S. Firstov, *et al.*, *J. Lightwave Technol.* **40**, 1161 (2022).
11. A. M. Khagai, S. V. Alyshev, A. S. Vakhrushev, *et al.*, *J. Non-Cryst. Solids: X* **16**, 100126 (2022).
12. S. V. Firstov, V. F. Khopin, I. A. Bufetov, *et al.*, *Opt. Express* **19**, 19551 (2011).
13. Z. Zhai, "Dataset in support of the journal article 'High-gain wideband bismuth-doped fiber amplifier operating in the O + E + S band'," University of Southampton, 2024, <https://doi.org/10.5258/SOTON/D2991>.